J1.1 Probing into Regional O_3 and PM Pollution: A 1-year CMAQ Simulation and Process Analysis over the United States

Yang Zhang[1], Krish Vijayaraghavan[2], Jian-Ping Huang[1], and Mark Z. Jacobson[3]

[1]Department of Marine, Earth and Atmospheric Sciences, North Carolina State University, Raleigh, NC

[2]Atmospheric & Environmental Research, Inc., San Ramon, CA

[3]Stanford University, Stanford, CA

1. INTRODUCTION

Regional ozone (O_3) and fine particulate matter ($PM_{2.5}$) air pollution has been one of the major environmental concerns in both the U.S. and abroad in the past several decades. While significant progress has been made to reduce emissions that contribute to the formation of O_3 and $PM_{2.5}$ and their concentrations have been declined steadily in recent years (U.S. Environmental Protection Agency (EPA), 2004 a, b, 2005), regional O_3 and $PM_{2.5}$ pollution continues to be a pervasive problem worldwide. For example, more than 159 million people in the U.S. are still living in nonattainment areas that do not meet the 8-hr O_3 standard (U.S. EPA, 2005). A better understanding of controlling factors of regional air pollution and more effective integrated emission control strategies are critical to the further improvement of ambient air quality.

Regional O_3 and $PM_{2.5}$ pollution may be caused by many factors including emissions, in-situ photochemistry, local meteorological processes, and interstate/intercontinental transport. A number of probing techniques have been developed to provide diagnostic evaluations of air quality models (AQMs) and to indicate the responses of model predictions to changes in emissions. An evaluation of several representative techniques such as those of mass-balance and sensitivity analyses for three-dimensional (3-D) AQMs has recently been conducted in Zhang et al. (2005 a). Process analysis (PA) is one of such tools that enable an in-depth understanding of the major contributors to the formation and fate of air pollutants. The PA calculates the Integrated Process Rates (IPRs) and the Integrated Reaction Rates (IRRs). The IPRs provide the change in species concentrations due to different physical and chemical processes (e.g., transport, emission, chemistry, aerosol and cloud processes, and deposition). The IRRs provide individual gas-phase reaction rates, permitting a detailed study of the chemical transformation of the species of interest such as O_3 and its precursors (Jeffries and Tonnesen, 1994; Jang et al., 1995).

In this study, a full year simulation with the U.S. EPA Models-3 Community Multiscale Air Quality (CMAQ) Modeling System and PA has been conducted for year 2001 over the contiguous U.S. Model predictions of gas and PM concentrations are evaluated against measurements from satellites and ground-based monitoring networks. The seasonal and annual photochemical characteristics over different regions are examined and the relative contributions of controlling processes are quantified for the formation and fate of key pollutants such as O_3, total odd oxygen (O_x = O_3 + nitrogen dioxide (NO_2) + 2 × nitrogen trioxide (NO_3) + oxygen atom (O) + excited-state oxygen atom (O^1D) + peroxyacyl nitrate (PAN) + 3 × dinitrogen pentoxide (N_2O_5) + nitric acid (HNO_3) + pernitric acid (HNO_4) + unknown organic nitrate), and $PM_{2.5}$.

2. DOMAIN AND MODEL CONFIGURATION

The CMAQ version 4.4 released in October 2004 (Binkowski and Roselle, 2003; Byun and Schere, 2005) has been applied to the contiguous U.S. with a horizontal grid resolution of 36-km. The modeling domain covers the contiguous U.S. and a portion of southern Canada and northern Mexico with 148 × 112 horizontal grid cells. The vertical resolution includes 14 logarithmic structure layers from the surface to the tropopause (at 15.676 km), with a finer resolution in the planetary boundary layer (PBL). The 14 layers correspond to the sigma levels of 0.995, 0.99, 0.98, 0.96, 0.94, 0.91, 0.86, 0.8, 0.74, 0.65, 0.55, 0.4, 0.2, 0.0. The first model layer height is set to be 35 m above the ground level (AGL).

The meteorological fields, emissions, initial conditions (ICONs), and boundary conditions

*Corresponding author address: Yang Zhang, Department of Marine, Earth and Atmospheric Sciences, Campus Box 8208, NCSU, Raleigh, NC 27695; e-mail: yang_zhang@ncsu.edu.

(BCONs) are provided by the U.S. EPA. The meteorological fields are generated using the Pennsylvania State University (PSU) / National Center for Atmospheric Research (NCAR) Mesoscale Modeling System Generation 5 (MM5) Version 3.6.1 with four-dimensional data assimilation (FDDA). The MM5 hourly output files are processed with the Meteorology-Chemistry Interface Processor (MCIP) version 2.2 for CMAQ. The EPA's National Emissions Inventories (NEI) 2001 (also referred to as NEI 1999 Version 3) is used to generate a gridded anthropogenic emission inventory for sulfur dioxide (SO_2), carbon monoxide (CO), nitric oxide (NO), nitrogen dioxide (NO_2), ammonia (NH_3), volatile organic compounds (VOCs), and PM. Emissions of VOCs, CO, nitrogen oxides (NO_x), and PM from mobile sources are generated with the latest onroad motor vehicle emissions model, MOBILE6 (U.S. EPA, 2003), and biogenic emissions are generated using the Biogenic Emissions Inventory System (BEIS) 3.12 (http://www.epa.gov/asmdnerl/biogen.html). The seasonality of the ammonia emissions is accounted for based on the results of Gilliland et al. (2003) and Pinder et al. (2004). The emission inventory is processed with the Sparse Matrix Operator Kernel Emissions system (SMOKE1.4). The initial conditions (ICONs) and boundary conditions (BCONs) are generated based on results from a global chemistry model of Bey et al. (2001) (i.e., GEOS-CHEM). A spin-up period of 10 days (December 22-31, 2000) is used to minimize the influence of ICONs.

The Carbon-Bond Mechanism version IV (CBM-IV) of Gery et al. (1989) and the Rosen Brock solver (ROS3) of Sandu et al. (1997) are used to simulate gas-phase chemistry. The aerosol module in CMAQ simulates major aerosol microphysics including thermodynamic equilibrium for both inorganic and organic species, binary nucleation of sulfuric acid and water vapor, coagulation, condensation, aerosol formation due to aqueous-phase chemistry, aerosol scavenged by cloud droplets, and dry and wet deposition. Particle size distribution is simulated with three lognormally-distributed modes: Aitken mode, accumulation mode, and coarse mode (correspond to particles with diameters up to approximately 0.1 μm, between 0.1 and 2.5 μm, and between 2.5 and 10 μm, respectively, for mass distribution). CMAQ uses a modified version of the aqueous-phase chemistry of Regional Acid Deposition Model (RADM) developed by Walcek and Taylor (1986). More detailed aerosol and cloud treatments can be found in Binkowski and Roselle (2003) and Bhave et al. (2004).

The process analysis is conducted using the PA tool for IRRs and IPRs imbedded in CMAQ. Hourly IPRs for 30 species (i.e., 11 individual gas-phase species, 7 lumped gas-phase species, and 12 lumped PM species) and IRRs for 96 gas-phase reactions in the CBM-IV mechanism are calculated from the surface to an altitude of 3.9 km (AGL) for the entire domain. The convergence tolerances of an absolute tolerance of 1×10^{-9} ppm and a relative tolerance of 1×10^{-3} are used to provide the accuracy requirements for computing IRR analysis for fast-reacting radicals such as OH and HO_2.

3. MODEL EVALUATION

Model evaluation is performed with both satellite and in-situ surface measurements using an evaluation protocol that follows Seigneur et al. (2000) and Zhang et al. (2005 b). The predicted total tropospheric O_3 column abundance from CMAQ and total aerosol optical depth (AOD) are compared with derived quantities based on satellite products from the Total Ozone Mapping Spectrometer (TOMS), the solar Backscattered Ultravoilet (SBUV) instruments, and the Moderate Resolution Imaging Spectroradiometer (MODIS). The max 1-hr and 8-hr average O_3 mixing ratios, and the 24-hr average mass concentrations of $PM_{2.5}$ and its composition are evaluated using the surface observational data from four nationwide routine monitoring networks: the Clean Air Status and Trends Network (CASTNet) (http://www.epa.gov/castnet/), the Interagency Monitoring of Protected Visual Environments (IMPROVE) (http://vista.cira.colostate.edu/improve/), the Aerometric Information Retrieval System (AIRS)-Air Quality System (AQS) (http://www.epa.gov/ air/data/ index.html), and the Speciation Trends Network (STN).

The evaluation protocol includes spatial distribution, temporal variation, and overall statistical trends. The statistical performance is evaluated with both traditional measures such as the mean normalized bias (MNB), the mean normalized gross error (MNGE), the normalized mean bias (NMB), and the normalized mean gross error (NMGE), as well as the newly-developed statistical metrics of Yu et al. (2005) such as the normalized mean bias factor (NMBF), and the normalized mean error factor (NMEF).

3.1 *Evaluation with Surface Measurements*

Table 1 summarizes the overall statistical performance of CMAQ for the max 1-hr and max 8-hr average O_3 mixing ratios at the CASTNet sites for the four seasons (DJF, MAM, JJA, and SON) and the full year of 2001. The model consistently underpredicts the max 1-hr O_3 mixing ratios by 7.9%, 0.8%, 2.4%, and 4.7% for DJF, MAM, JJA, and SON, respectively, resulting in an annual average underprediction of 3.4%. For the max 8-hr average O_3, the model underpredicts by 4.4% in DJF, overpredicts by 2.7% and 3.3% in MAM and JJA, respectively, and gives good agreement in SON (with a NMB of 0.05%), resulting in a net annual average overprediction of 1%. Those statistics are calculated using data paired-in-space only. Biases using data paired in both space and time may be higher. The latest U.S. EPA's guidance on the attainment demonstrations for the 8-hr O_3 NAAQS (U.S. EPA, 2005) indicates that it is not appropriate to assign 'bright line' criteria that distinguish between adequate and inadequate model performance. The performance of the seasonal and annual O_3 predictions of CMAQ is satisfactory based on the U.S. EPA's previous reports on the guidance on the attainment of 1-hr and 8-hr O_3, in which the values of MNB and MNGE recommended by EPA for a good performance of O_3 are ≤ 15% and ≤ 30%, respectively, and O_3 peak accuracy < 20%.

$PM_{2.5}$ and its composition are evaluated using data from IMPROVE, STN, and CASTNet. Table 2 summarizes the overall statistical performance for 24-hr average $PM_{2.5}$ at IMPROVE and STN sites for the four seasons and the full year. At IMPROVE sites, $PM_{2.5}$ concentrations are overpredicted by 30% in DJF and 13% in SON but underpredicted by 7% in MAM and 14% in JJA. The positive and negative biases compensate, resulting in only 1% annual average overprediction. At STN sites, small overpredictions occur in DJF, MAM, and SON (5-9%) and a small underprediction occurs in JJA (4%), resulting in a net 4% annual average overprediciton. Seigneur (2001) recommended a value of MNB of 50% or less for a satisfactory model performance for 24-hr average $PM_{2.5}$, based on current modeling practice that typically uses MNB/MNGE for model evaluation. The values of MNB and MNGE recommended by EPA as lower limits for a good performance of PM are ≤ 15% and ≤ 30%, respectively (U.S. EPA, 2001). While the values of MNB/MNGE and NMB/NMGE are similar in many cases, they may give different results in some cases (e.g., when the observed values at a specific time or location are extremely low), in such cases, the use of NMB/NMGE will provide a more reasonable evaluation. In this work, a cutoff of 0.5 μg m^{-3} is used to screen out extremely small observed values from those networks. All MNBs or NMBs or NMBFs > 0.15 and MNGEs or NMEs or NMBEs > 0.3, therefore, are considered here to indicate a relatively poor performance (as shaded in light gray color in Table 2). As shown in Table 2, the statistical results with various metrics are quite consistent. The performance of $PM_{2.5}$ predictions is generally poor with NMEs of 37-59% for seasonal and annual predictions at both networks and a NMB of 30% in DJF at IMPROVE sites. Analyses of statistics for $PM_{2.5}$ composition predictions indicate a worse performance for NH_4^+ and NO_3^- at IMPROVE sites (primarily remote locations), with NMBs of -11% to 19% for SO_4^{2-}, 20-41% for NH_4^+, -15% to 37% for NO_3^-, -17% to -28% for BC, and 0-4% for OC; and a much worse performance at STN sites (all urban locations), with NMBs of -28% to 8% for SO_4^{2-}, -42 to -19% for NH_4^+, -85% to -27% for NO_3^-, -66 to -52% for BC, and -60% to -42% for OC.

3.2 *Evaluation with Satellite Measurements*

3-D gridded hourly average O_3 mixing ratios are simulated using CMAQ up to an altitude of about 15 km AGL. These simulated O_3 mixing ratios and MM5-predicted vertically-resolved temperature and pressure are used to calculate the total tropospheric O_3 column abundance (TOCA) in Dobson units (DUs) as follows:

$$TOCA = \sum_{l=1}^{14} \frac{p_l \times \Delta z_l \times A \times [O_3]_{ppm,l}}{R \times T_l \times 10^6 \times C_{DU}} \qquad (1)$$

where $[O_3]_{ppm,l}$ is the O_3 mixing ratio in ppm in layer l, Δz_l is the height of layer l in m, p_l and T_l are the pressure in Pa and temperature in K, respectively, in layer l, R is the gas constant (= 8.34 J $mole^{-1}$ K^{-1}), A is the Avogadro's number (= 6.02213 ×10^{23} molecules $mole^{-1}$), and C_{DU} is the conversion factor from molecules O_3 m^{-2} to DU (= 2.687×10^{22}). Monthly, seasonal, and annual averages are computed for each grid cell. The simulated TOCAs are compared with the tropospheric O_3 residuals (TORs) derived from TOMS and SBUV described in Fishman et al. (2005). The TOMS aboard the Earth Probe satellite was experiencing instrumental problems in early 2001, the monthly-mean TOR values are thus only available for Jan., Feb., and Mar. 2001 for comparison.

Figure 1 shows the simulated monthly-mean TOCAs and derived TORs in DUs for Jan., Feb., and Mar., 2001. Among the three months, the derived TORs are the smallest in Jan. and the largest in Mar. This variation is well reproduced by CMAQ, despite appreciable differences between TORs and TOCAs in certain regions. The total O_3 column abundances over the modeling domain typically are 15-46 DUs in Jan., 15-50 DUs in Feb., and 15-56 DUs in Mar. Those values are generally consistent with the derived TORs with the best agreement in Jan. Overpredictions of ~10 DUs occur in the eastern portion of the domain and underpredictions of ~10-20 DUs occur in the western portion of the domain.

4. PROCESS ANALYSIS

Detailed IPR and IRR analyses are performed at 16 locations that represent air masses of different origins (e.g., urban vs. rural, inland vs. coast, NO_x-limited vs. VOC-limited regions). The 16 locations include Big Bend NP (BBE), TX; Chicago (CHI), IL; Fresno (FRE), CA; Grand Canyon National Park (GRC), AZ; Great Smoky National Park (GRS), TN; Huston, TX; Atlanta (ATL), GA; Los Angeles (LAX), CA; New York city (NYC); Olympic National Park (OLY), WA; Pittsburgh (PIT), PA; Penn State (PSU), PA; Riverside (RIV), CA; Yellowstone National Park (YEL), WY; and Yorkville (YRK), GA; and Tampa (TAM), FL.

4.1 Integrated Process Rates (IPRs)

Figure 2 shows the hourly O_3 change in ppb at TAM and LAX in surface layer on March 24 and June 7 2001 during which the peak O_3 mixing ratio is the highest among all days in each month. At both locations, vertical transport plays a dominant role in transporting O_3 from adjacent cells into the two locations. Dry deposition is a predominant pathway at TAM and an important pathway at LAX to remove O_3. Horizontal transport either increases or decreases O_3; it causes more O_3 changes at LAX than at TAM. Gas-phase chemistry contributes to O_3 production between 11 a.m. to 4 p.m., easterner standard time (EST) at TAM on March 24 and June 7 and at LAX on June 7, but to O_3 destruction (via NO titration) during other hours. Significant NO titration occurs at LAX on March 24 due to a large source of NO_x emissions, resulting in a negative chemistry contribution to O_3 formation throughout the day. At both locations, photochemical production and destruction of O_3 are stronger on June 7 than March 24. The mass adjustment contributes to larger O_3 changes at LAX than at TAM on both days, indicating that solving either advection or gas-phase chemistry or both may be more difficult (i.e., the numerical equations for those processes are stiffer) under ambient conditions at LAX, probably due to either a more complex terrain or higher concentrations and faster chemical reaction rates, or both.

Figure 3 shows the daily contributions of individual processes to the mass concentrations of $PM_{2.5}$, fine ammonium ($NH4_{2.5}$), fine sulfate ($SO4_{2.5}$), fine nitrate ($NO3_{2.5}$), fine primary organic matter ($POM_{2.5}$), fine secondary organic matter ($SOM_{2.5}$), other fine unknown PM ($OIN_{2.5}$), and fine BC ($BC_{2.5}$) on June 7 at LAX. At LAX, emission is the largest contributor to the concentrations of $PM_{2.5}$ and all PM species except for $NO3_{2.5}$ and $NH4_{2.5}$. Vertical transport decreases the concentrations of $PM_{2.5}$ and its composition (except $NO3_{2.5}$ and $SOM_{2.5}$) for most hours via mixing and ventilation of these species. Horizontal transport either increases or decreases all species concentrations, as it carries these pollutants into or out of the location. Aerosol processes (e.g., chemical equilibrium, condensation/evaporation, and coagulation) cause an increase in the mass concentrations of secondary PM species such as $NO3_{2.5}$, $NH4_{2.5}$, and $SOA_{2.5}$ (thus $PM_{2.5}$) before 9 a.m. and after 8 p.m., but a concentration decrease between 9 a.m. and 8 p.m. The contributions of dry deposition and cloud processes (i.e., aqueous-phase chemistry and wet deposition) to the changes in the concentrations of $PM_{2.5}$ and its composition are negligible at LAX on June 7.

4.2 Integrated Reaction Rates (IRRs)

Figure 4 shows the spatial distribution of seasonal-mean total O_x production at layer 1. The production of O_x is the highest in JJA, followed by SON, MAM, and DJF, indicating an overall higher oxidation capacity in summer and fall. During summer and fall, higher production occurs over several states in the western U.S. including California, Arizona, New Maxico, Colorado, Utah, and Oregon, over several states in the southeastern U.S. including Florida, Georgia, Alabama, South Carolina, and North Carolina, over the states of Montana, Texas, and Louisiana, as well as northern Mexico. Figure 5 shows the seasonal and annual production and the loss rates of O_x in the surface layer at four urban sites (i.e., CHI, LAX, ATL, and NYC), a suburban site (i.e., RIV), and a rural location (i.e., YRK). At all locations, O_x production is the highest in summer, followed by fall or spring, then winter. Among the

six locations, the net summer production of O_x is the highest at JST, followed by LAX, YRK, CHI, NYC, and RIV. Figure 6 shows the rate of OH reacted with anthropogenic and biogenic volatile organic compounds (AVOCs and BVOCs, respectively) at the six locations. The highest rates of OH reacted with both AVOCs and BVOCs occur at ATL. The rate of OH reacted with BVOCs is even higher than that with AVOCs at YRK during summertime. ATL and YRK are representative urban and rural locations, respectively, in the southeastern U.S., where O_3 chemistry is characterized by NO_x-limited conditions, due to high BVOC emissions (Zhang et al., 2005 c). The stagnant and hot summer conditions inhibit the dispersion of pollutants and favor the accumulation of O_3 and PM precursors near the surface. LAX and RIV represent southwestern urban and suburban locations, respectively, with a VOC-limited chemistry. Nearly the same rates of OH reacted with both AVOCs and BVOCs at LAX, whereas the rate of OH reacted with BVOCs is much smaller than that with AVOCs at RIV, reflecting much lower BVOC emissions at RIV. In this region, temperature is typically high but relative humidity (RH) is typically low inland during the day in the summertime. Fogs occur most frequently during mid-night and in the morning, facilitating the formation of secondary PM (as shown in Figure 3). NYC represents a northeastern urban location, where the climatology is characterized by a warm temperature, high RH, coupled with pollutant transport along the axis of major source areas (Zhang et al., 2005 a). The O_3 chemistry can be either VOC- or NO_x-limited. The seasonal and annual rates of OH reacted with BVOCs are the lowest among the four urban locations. CHI represents an urban location in the midwestern U.S. with a high temperature, a medium RH, and a VOC-limited chemistry in the summertime. The rate of OH reacted with AVOCs is stronger than that with BVOCs.

5. SUMMARY AND FUTURE WORK

Model evaluation has shown a good overall performance for max 1-hr and 8-hr average O_3 mixing ratios and a relatively poor performance for 24-hr average $PM_{2.5}$ concentrations. The performance of CMAQ is generally consistent with current PM model performance, however, with worst performance over urban areas (i.e., at the STN sites) and relatively high NMBs in nitrate, ammonium, BC, and OC. The total tropospheric O_3 column abundances predicted by CMAQ give a relatively good agreement with the tropospheric O_3 residuals, consistent with a good agreement between simulated and observed surface O_3 mixing ratios. CMAQ v4.4 does not calculate AOD. In this study, we have calculated offline the monthly-mean AOD based on PM predictions of CMAQ using an empirical approach of Chameides et al. (2002) (figures not shown here, see Zhang et al., 2005 d). We have also incorporated an online AOD module that is based on a Mie parameterization. The simulated AODs are being compared with observations from MODIS.

Uncertainties and likely causes for discrepancies between simulated and observed $PM_{2.5}$ will be analyzed and identified. The total masses of major air pollutants such as O_x and $PM_{2.5}$ exported from the urban/regional scale to the global atmosphere are being estimated via budget analyses. A set of sensitivity simulations will be conducted to study the effect of urban/regional emissions on the large-scale environment. The relative importance of individual VOCs (e.g., isoprene) in controlling the fate of O_3 and aerosols leaving the urban/regional scale will be evaluated. The effect of model physics (e.g., cloud chemistry and plume-in-grid treatment) and grid resolution on the export of O_3, aerosols, and their precursors such as NO_x and VOCs, from the urban/regional scale will also be examined.

Acknowledgements

This work is performed under the National Aeronautics and Space Administration Award No. NNG04GJ90G. The authors thank Jack Fishman and John K. Creilson, NASA Langley Research Center, for providing Tropospheric Ozone Residual data; Shaocai Yu, U.S. EPA/NOAA, for providing FORTRAN script for statistical calculations; Shiang-Yuh Wu, Department of Environmental Quality, the state of Virginia, for her assistance in TOR data processing.

6. REFERENCES

Bey, I., D. J. Jacob, R. M. Yantosca, J. A. Logan, B. D. Field, A. M. Fiore, Q. Li, H. Y. Liu, L. J. Mickley, and M. G. Schultz, 2001: Global modeling of tropospheric chemistry with assimilated meteorology: Model description and evaluation. *J. Geophys. Res.*, **106**(D19), 23073-23096, 10.1029/2001JD000807.

Bhave, P.V., Roselle, S.J. , Binkowski, F.S., Nolte, C.G., Yu, S., Gipson, G.L., and Schere, K.L., 2004: CMAQ aerosol module development: recent enhancements and future plans, presented at the

2004 Models-3 Users Workshop, Chapel Hill, North Carolina, October 18–20.

Binkowski, F.S., and S.J. Roselle, 2003: Models-3 community multiscale air quality (CMAQ) model aerosol component, 1. Model description. *J. Geophys. Res.*, **108**, 4183, doi:10.1029/2001JD001409.

Byun, D., and Schere, K.L., 2005: Review of the Governing Equations, Computational Algorithms, and Other Components of the Models-3 Community Multiscale Air Quality (CMAQ) Modeling System. *Applied Mechanics Reviews* (in press).

Chameides, W.L., C. Luo, R. Salor, D. Streets, Y. Huang, M. Bergin, and F. Giorgi, 2002: Correlation between model-calculated anthropogenic aerosols and satellite-derived cloud optical depths: Indication of indirect effect? *J. Geophys. Res.*, **107** (D10), 10.1029/2000JD000208.

Fishman, J., A.E. Wozniak, and J.K. Creilson, 2003: Global distribution of tropospheric ozone from satellite measurements using the empirically corrected tropospheric O_3 residual techniques: identification of the regional aspects of air pollution. *Atmos. Chem. Phys.*, **3**, 893-907.

Gery, M.W., G.Z. Whitten, J.P. Killus, and M.C. Dodge, 1989: A photochemical kinetics mechanism for urban and regional scale computer modeling. *J. Geophys. Res.*, **94**, 12,925-12,956.

Gilliland A.B., R. L. Dennis, S. J. Roselle, and T. E. Pierce, 2003, Seasonal NH_3 emission estimates for the eastern United States based on ammonium wet concentrations and an inverse modeling method. *J. Geophys. Res.*, **108** (D15), 4477, doi:10.1029/2002JD003063.

Jang J.-C. C., H.E. Jeffries and S. Tonnesen, 1995: Sensitivity of ozone to model grid resolution – II. Detailed process analysis for ozone chemistry. *Atmos. Environ.,* **29**, 3101-3114.

Jeffries, H.E. and S. Tonnesen, 1994: A comparison of two photochemical reaction mechanisms using mass balance and process analysis, *Atmos. Environ.*, **28**, 2991-3003.

Pinder R.W., R. Strader, C.I. Davidson and P.J. Adams, 2004: A temporally and spatially
resolved ammonia emission inventory for dairy cows in the United States. *Atmos. Environ.,* **38**, 3747-3756.

Sandu, A., J. G. Verwer, J. G., Blom, E. J. Spee, G. R. Carmichael, and F. A. Potra, 1997: Benchmarking stiff ODE solvers for atmospheric chemistry problems II: Rosenbrock solvers. *Atmos. Environ.*, **31**, 3459-3472.

Seigneur, C., 2001: Current status of air quality models for particulate matter. *J. Waste Manage. Assoc.*, **51**, 1508-1521.

Seigneur, C., B. Pun, P. Pai, J.F. Louis, P. Solomon, C. Emery, R. Morris, M. Zahniser, D. Worsnop, P. Koutrakis, W. White, and I. Tombach, 2000: Guidance for the performance evaluation of three-dimensional air quality modeling systems for particulate matter and visibility, *J. Waste Manage. Assoc.*, **50**, 588-599.

U.S. EPA, 2001: Draft guidance for demonstrating attainment of air quality goals for $PM_{2.5}$ and regional haze, U.S. Environmental Protection Agency, Research Triangle Park, NC.

U.S. EPA, 2003: User's guide to MOBILE6.1 and MOBILE6.2; EPA Office of Air and Radiation, EPA420-R-03-010, Assessment and Standards Division, Office of Transportation and Air Quality, U.S. Environmental Protection Agency, Research Triangle Park, NC. 262pp.

U.S. EPA, 2004a: The ozone report: measuring progress through 2003, Office of Air Quality Planning and Standards, the U.S. Environmental Protection Agency, EPA-454-K-04-001, Research Triangle Park, NC, April.

U.S. EPA, 2004b: The particle pollution report: current understanding of air quality and emissions through 2003, Office of Air Quality Planning and Standards, the U.S. Environmental Protection Agency, EPA-454-K-04-002, Research Triangle Park, NC, December.

U.S. EPA, 2005: Evaluating ozone control programs in the eastern United States: NOx budget trading program progress and compliance, Office of Air and Radiation/Office of Air Quality Planning and Standards/Office of Atmospheric Programs, the U.S. Environmental Protection Agency, EPA-454-K-05-001, Washington, DC, June.

Walcek, C.J. and G.R. Taylor, 1986: A theoretical method for computing vertical distributions of acidity and sulfate production within cumulus clouds. *J. Atmos. Sci.*, **43**, 339-355.

Yu, S., B.K. Eder, R. Dennis, S.-H. Chu, and S. Schwartz, 2005: New unbiased symmetric metrics for evaluation of air quality models, *Atmos. Environ.*, in review.

Zhang, Y., K. Vijayaraghavan, and C. Seigneur, 2005 a: Evaluation of three probing techniques in a three-dimensional air quality model, *J. Geophys. Res.*, **110**, D02305, doi:10.1029/2004JD005248.

Zhang, Y., P. Liu, B. Pun, and C. Seigneur, 2005 b: A Comprehensive Performance Evaluation of MM5-CMAQ for Summer 1999 Southern Oxidants Study Episode, Part I. Evaluation Protocols, Databases and Meteorological Predictions, *Atmos. Environ.*, in review.

Zhang, Y., Liu, P., Queen, A., Misenis, C., Pun, B., Seigneur, C., Wu, S.-Y., 2005 c: A Comprehensive Performance Evaluation of MM5-CMAQ for Summer 1999 Southern Oxidants Study Episode, Part II. Gas and Aerosol Predictions. *Atmos. Environ.*, in review.

Zhang, Y., H. E. Snell, K. Vijayaraghavan, and M.Z. Jacobson, 2005 d: *Evaluation of Regional PM Predictions with Satellite and Surface Measurements*, presented at the 24th Annual Meeting of American Association for Aerosol Research, October 17-21, Austin, Texas.

Table 1. Quantitative performance statistics for the predicted surface O_3 mixing ratios for year 2001 against observations from CASTNet.

Variables[1]	**Max 1-hr O_3**					**Max 8-hr O_3**				
	DJF	MAM	JJA	SON	Annual	DJF	MAM	JJA	SON	Annual
Mean Obs., ppb	36.26	54.03	58.89	46.30	49.03	31.90	48.44	51.09	39.97	42.97
Mean Sim., ppb	33.40	53.58	57.49	44.14	47.36	30.51	49.74	52.79	39.99	43.40
Total #	5710	6008	6099	6179	23996	7938	8439	8396	8501	33274
Corr. Coeff.	0.52	0.60	0.60	0.59	0.67	0.68	0.69	0.64	0.68	0.76
MNB	-0.03	0.02	0.02	0.01	0.01	0.03	0.06	0.09	0.09	0.06
MNGE	0.21	0.15	0.18	0.18	0.18	0.26	0.17	0.22	0.24	0.22
NMB	-0.08	-0.01	-0.02	-0.05	-0.03	-0.04	0.03	0.03	0.00	0.01
NME	0.19	0.14	0.17	0.17	0.17	0.20	0.15	0.18	0.19	0.18
NMBF	-0.09	-0.01	-0.02	-0.05	-0.04	-0.05	0.03	0.03	0.00	0.01
NMEF	0.21	0.14	0.17	0.18	0.17	0.21	0.15	0.18	0.19	0.18

1. MNB - the mean normalized bias; MNGE - the mean normalized gross error; NMB - the normalized mean bias; NME - the normalized mean error; NMBF - the normalized mean bias factor; and NMEF - the normalized mean error factor.

Table 2. Quantitative performance statistics for the predicted surface $PM_{2.5}$ concentrations for year 2001 against observations from IMPROVE and STN.

Variables[1,2]	**IMPROVE**					**STN**				
	DJF	MAM	JJA	SON	Annual	DJF	MAM	JJA	SON	Annual
Mean Obs., $\mu g\ m^{-3}$	3.95	5.90	7.79	5.60	5.88	12.86	11.58	14.06	12.45	12.83
Mean Sim., $\mu g\ m^{-3}$	5.13	5.50	6.66	6.33	5.95	13.47	12.35	13.53	13.53	13.28
Total #	2843	3255	3370	3658	13126	1054	1116	1638	1736	5544
Corr. Coeff.	0.68	0.67	0.75	0.73	0.71	0.39	0.56	0.66	0.57	0.55
MNB	0.66	0.10	0.01	0.31	0.26	0.37	0.22	0.09	0.25	0.22
MNGE	0.86	0.50	0.47	0.56	0.59	0.71	0.52	0.44	0.53	0.53
NMB[3]	0.30	-0.07	-0.14	0.13	0.01	0.05	0.07	-0.04	0.09	0.04
NME[3]	0.59	0.44	0.40	0.45	0.45	0.53	0.43	0.37	0.45	0.44
NMBF	0.30	-0.07	-0.17	0.13	0.01	0.05	0.07	-0.04	0.09	0.04
NMEF	0.59	0.47	0.46	0.45	0.45	0.53	0.43	0.38	0.45	0.44

1. MNB - the mean normalized bias; MNGE - the mean normalized gross error; NMB - the normalized mean bias; NME - the normalized mean error; NMBF - the normalized mean bias factor; and NMEF - the normalized mean error factor.
2. The statistics are obtained for any pairs of the simulated and observed concentrations of PM_{10}, $PM_{2.5}$ and $PM_{2.5}$ composition when the observed mass concentration was > 0.5 $\mu g\ m^{-3}$.
3. All MNBs or NMBs or NMBFs > 0.15 and NMEs or MNGEs, or NMEFs > 0.30 are considered in this work to indicate relatively poor performance and are highlighted with the shaded light gray color.

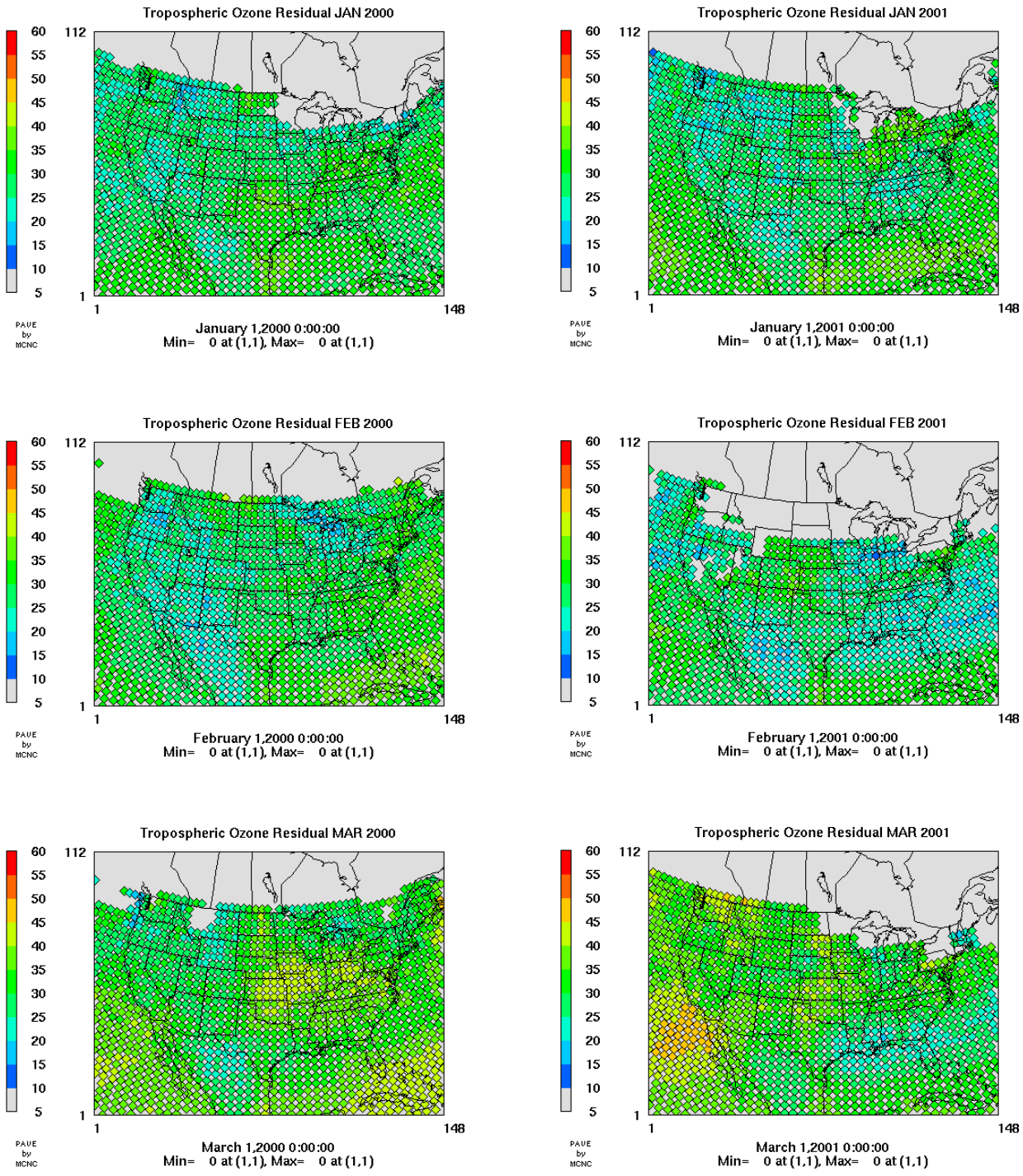

Figure 1. The tropospheric O_3 column abundance (TOCAs) predicted by CMAQ (left column) and the tropospheric O_3 residuals derived from TOMS and SBUV (right-column) in DUs in Jan., Feb., and Mar., 2001.

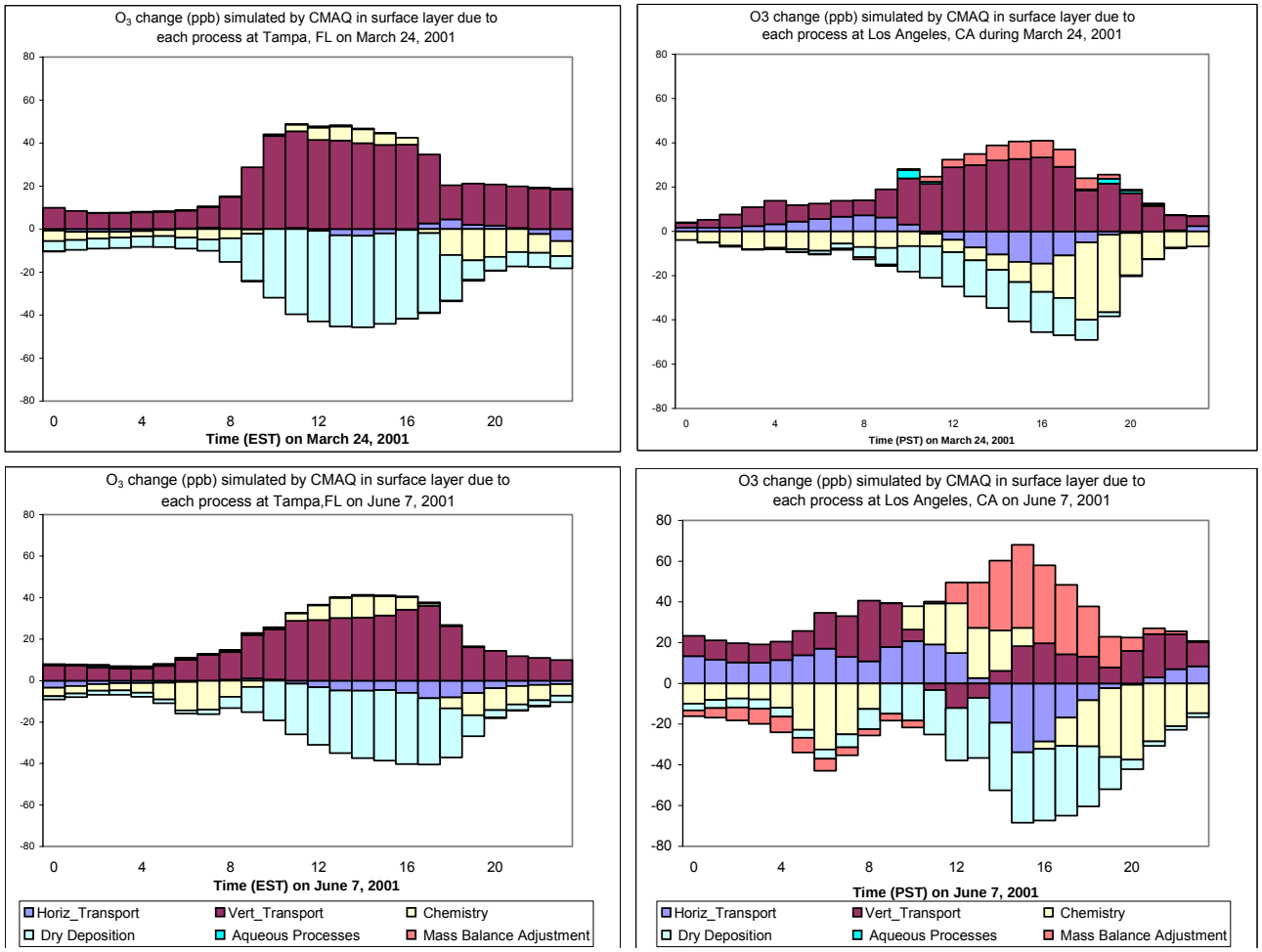

Figure 2. The hourly O_3 change in ppb at TAM and LAX in surface layer on March 24 and June 7 2001 during which the peak O_3 mixing ratio was the highest among all days in each.

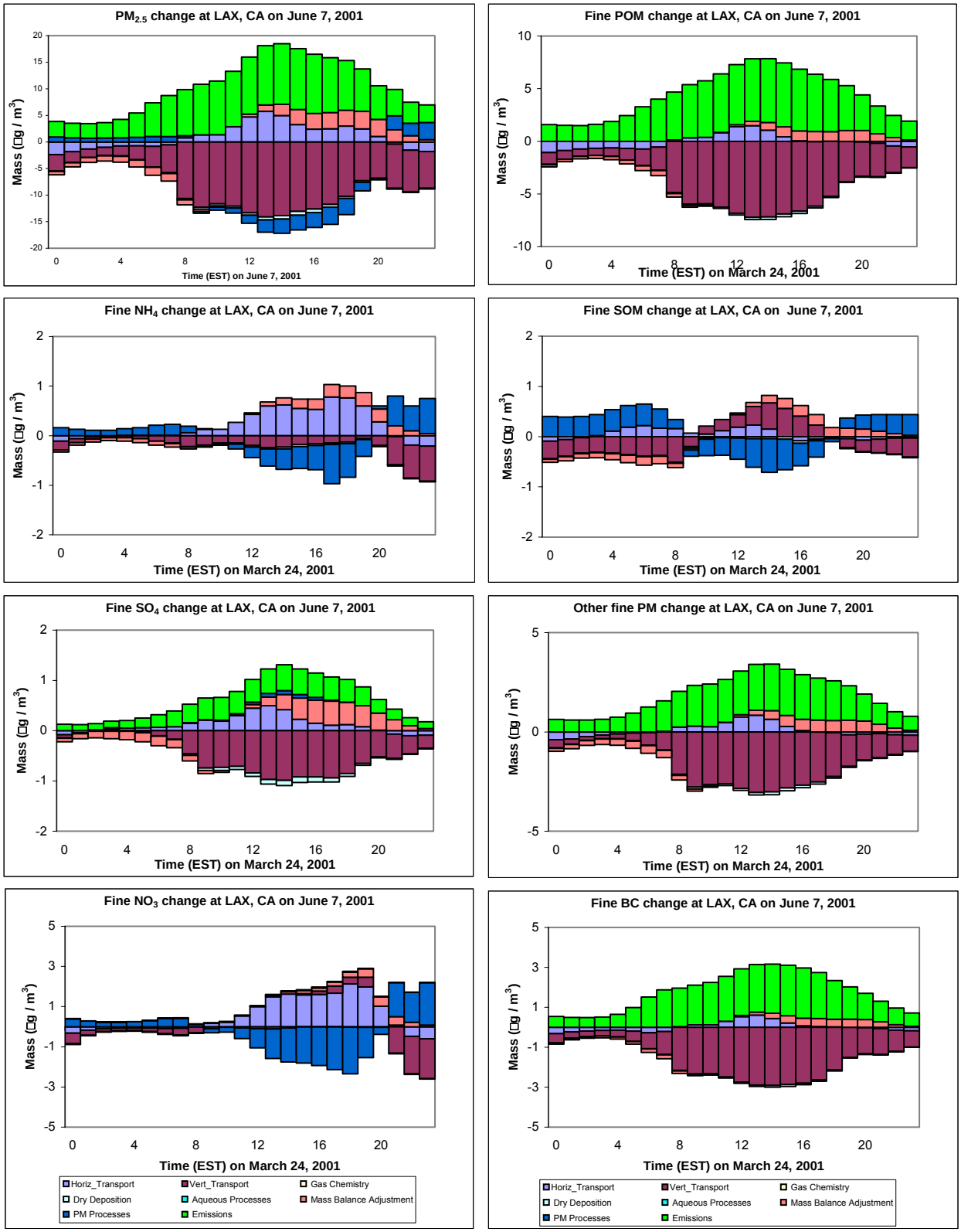

Figure 3. The daily contributions of individual processes to the mass concentrations of $PM_{2.5}$ and its composition at LAX on June 7 2001.

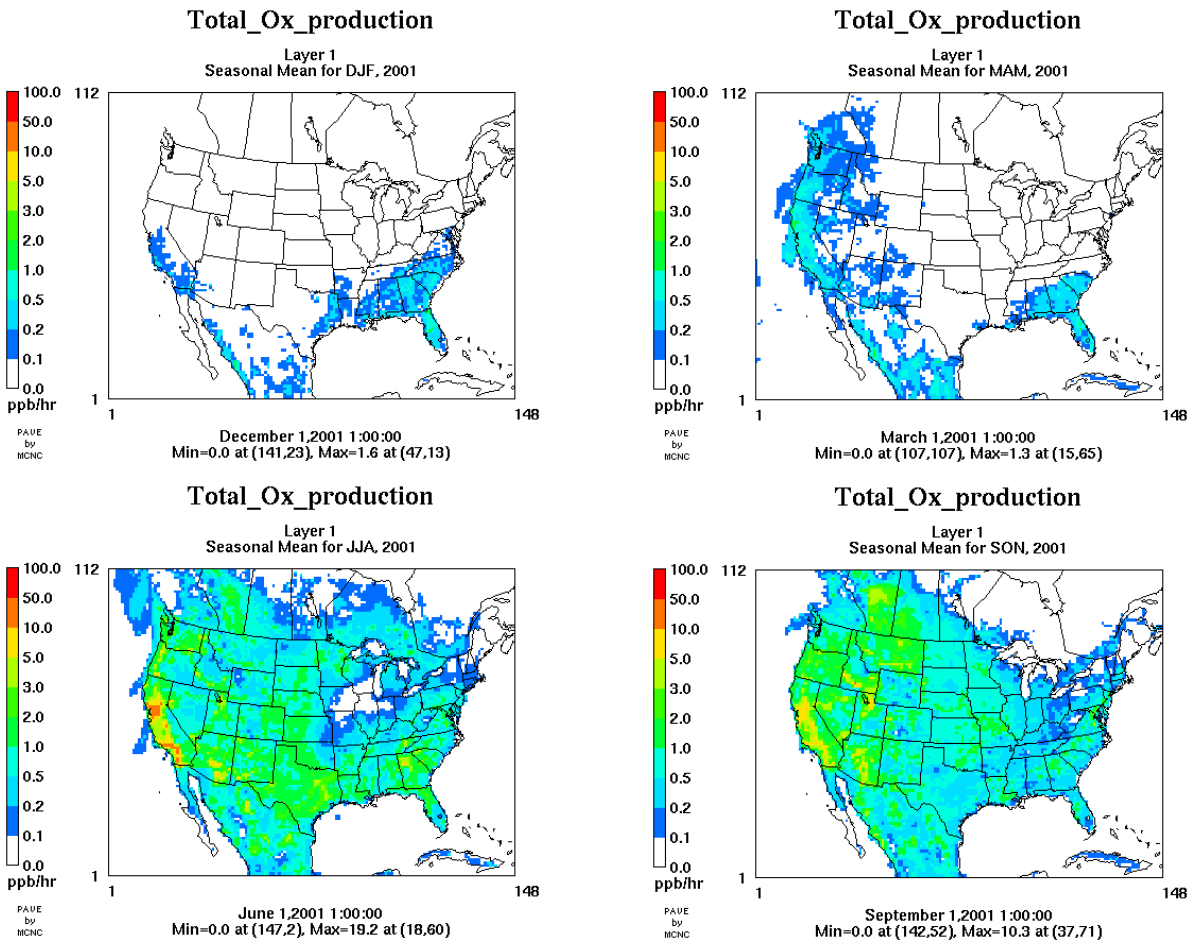

Figure 4. The monthly-mean spatial distribution of total O_x production in surface layer in year 2001.

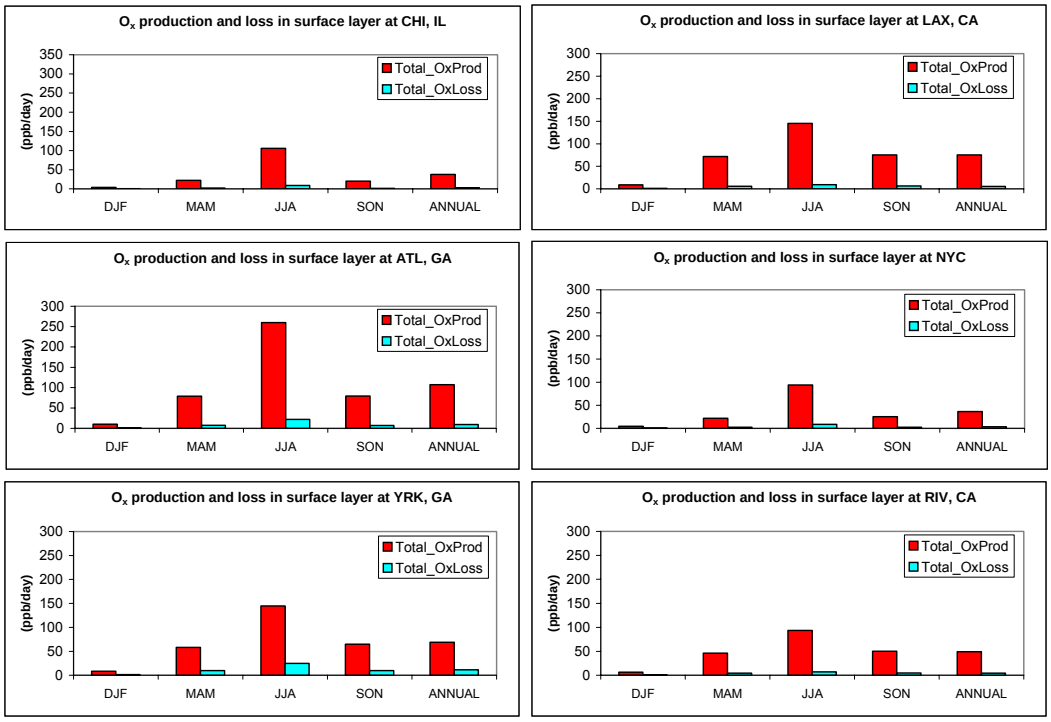

Figure 5. The seasonal- and annual-mean total O_x production and loss at Chicago (CHI), IL; Los Angeles (LAX), CA; Atlanta (ATL), GA; New York city (NYC); Yorkville (YRK), GA, and Riverside (RIV), CA.

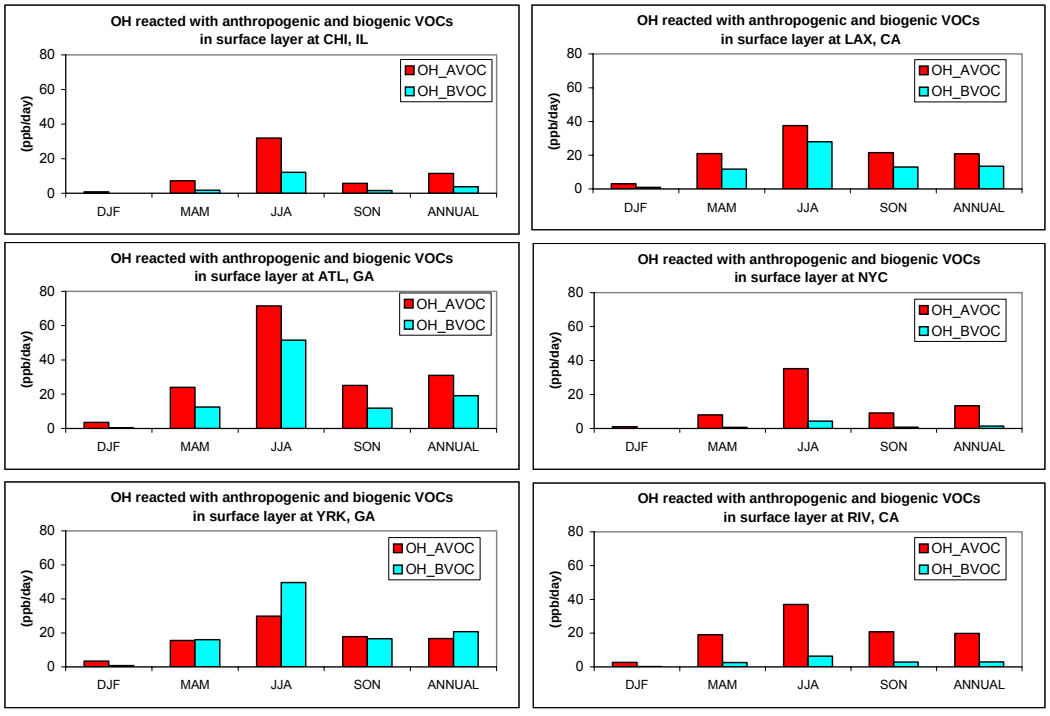

Figure 6. The seasonal- and annual-mean rates of OH reacted with anthropogenic and biogenic VOCs at Chicago (CHI), IL; Los Angeles (LAX), CA; Atlanta (ATL), GA; New York city (NYC); Yorkville (YRK), GA, and Riverside (RIV), CA.